

An efficient TiO₂ thin-film photocatalyst: photocatalytic properties in gas-phase acetaldehyde degradation

Iis Sopyan^a, Mitsuru Watanabe^b, Sadao Murasawa^b, Kazuhito Hashimoto^a,
Akira Fujishima^{a,*}

^a Department of Applied Chemistry, Faculty of Engineering, The University of Tokyo, 7-3-1 Hongo, Bunkyo-ku, Tokyo 113, Japan

^b Central Research Institute, Ishihara Sangyo Kaisha Ltd., 2-3-1 Nishi-Shibukawa, Kusatsu, Shiga 525, Japan

Received 6 October 1995; accepted 1 February 1996

Abstract

A semitransparent TiO₂ film with extraordinarily high photocatalytic activity was prepared on a glass substrate by sintering a TiO₂ sol at 450 °C. Crystallographic analysis by X-ray diffraction and Raman spectroscopy showed that the film was purely anatase. The photocatalytic properties of the film were investigated by measuring the photodegradative oxidation of gaseous acetaldehyde at various concentrations under strong and weak UV light irradiation conditions. The photocatalytic activity of the film was higher than that of one of the most active commercial TiO₂ powders, Degussa P-25. The kinetics of acetaldehyde degradation as catalyzed by the TiO₂ film as well as by P-25 powder were analyzed in terms of the Langmuir–Hinshelwood model. It is shown that the number of adsorption sites per unit true surface area is larger with the TiO₂ film, as analyzed in the powder form, than with P-25 powder. Meanwhile, the first-order reaction rate constant is also much larger with the film than with P-25 powder. Moreover, under most experimental conditions, particularly with high concentrations of acetaldehyde and weak UV illumination intensity, the quantum efficiency was found to exceed 100% on an absorbed-photon basis, assuming that only photo-generated holes play a major role in the reaction. This leads to the conclusion that the photodegradative oxidation of acetaldehyde is not mediated solely by hydroxyl radicals, generated via hole capture by surface hydroxyl ions or water molecules, but also by photocatalytically generated superoxide ion, which can be generated by the reduction of adsorbed oxygen with photogenerated electrons.

Keywords: TiO₂ film; Active photocatalyst; Acetaldehyde degradations

1. Introduction

The photo-oxidative decomposition of organic compounds in colloidal and particulate semiconductor catalyst suspensions has been well studied. This process is based on the strong oxidative power of photogenerated holes on the photocatalyst surface [1–3]. However, several practical problems with using powders in photochemical processing are apparent: (1) separation of the catalyst from the suspension after the reaction is difficult, (2) the suspended particles tend to aggregate, especially when they are present at high concentrations, and (3) particulate suspensions are not easily applicable to continuous flow systems. In order to avoid these technical problems, several approaches have been taken. For example: (1) powder-type photocatalysts have been immobilized on various supports, including glasses [4], silica [5], polymers [5–9], clays [10], surfactant vesicles [11,12], and

micelles [13]; and (2) catalysts were prepared in film form [4,14–27]. Although these approaches have not been completely successful, the development of immobilized photocatalysts with high activity is still of great technological importance. However, film-type photocatalysts normally have lower surface areas than powdered ones, and the intrinsic photocatalytic activity of films is usually smaller than that of powders.

Recently we have developed a procedure for the preparation of TiO₂ thin films with high photocatalytic activity. We found that a TiO₂ film coated on a flat substrate by sintering an anatase sol exhibited efficient photocatalytic decomposition of acetaldehyde even with room light illumination. Surprisingly, it was observed that the film showed much higher photocatalytic activity than that of one of the most active commercial TiO₂ powders, Degussa P-25 [28].

This paper addresses the detailed characterization and investigation of the photocatalytic activity of this extraordinarily active TiO₂ film, and includes comparisons with P-25 powder. The photoactivities were measured as the photode-

* Corresponding author. Phone: +81 3 3812 2111, Ext. 7245; Fax: +81 3 3812 6227.

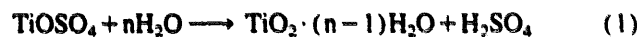
composition rates of gaseous acetaldehyde as a function of the UV light intensity and the reactant concentrations. The adsorption of acetaldehyde in the dark is examined in terms of the Langmuir isotherm, and the kinetics of the photolytic reactions are examined in terms of the Langmuir–Hinshelwood (L–H) model. Finally, several reasonable reaction mechanisms are proposed that are consistent with the measured quantum yields.

2. Experimental details

2.1. Materials

All of the chemicals used were reagent-grade. Acetaldehyde was purchased from Merck Japan Co. Ltd. For purposes of comparison, TiO₂ powder catalyst, Degussa P25 (anatase, Nippon Aerosil Co., Tokyo), with an average particle size of 30 nm and BET surface area of 50 m² g⁻¹ were used as received. The light source used was a 500 W high-pressure Hg lamp (Ushio Co. Ltd., Model USH-500D), together with a band-pass filter at 365 nm (Melles–Griot 03F1MO28), which had a transmission bandwidth at half-maximum of 4.5 nm. The UV intensity was controlled by using neutral-density filters.

The preparation procedure for the TiO₂ thin film has been previously reported [28]. It involves the preparation of a titanate acid sol via the thermal hydrolysis of an aqueous titanate sulfate solution



followed by dispersion with nitric acid to form the titanate acid sol. In order to enhance its crystallinity, this sol was then autoclaved at 180 °C for 30 min. The autoclaved TiO₂ sol is now commercially available (Ishihara Sangyo Kaisha Ltd., ST-11). The BET surface area of the TiO₂ powder obtained by drying the sol was 64 m² g⁻¹. Hereafter, the TiO₂ powder obtained is referred to as "TiO₂ powder A". A coating of the TiO₂ sol was applied to a fused silica plate substrate (6 cm × 8 cm × 1 mm) followed by sintering at 450 °C in air for 30 min. An X-ray diffraction pattern of the film on the glass substrate was obtained for 2θ diffraction angles between 20 and 60° using a Rigaku Denki Model RINT-2400. The Raman spectrum was recorded on a Renishaw Ramascope using an argon-ion laser (514.5 nm) as the light source, with an exposure time of 10.0 s. Scanning electron microscopic (SEM) examination of the film was carried out on a Hitachi Co. Ltd. Model S-530.

2.2. Adsorption isotherm analysis

The adsorption–desorption equilibrium of acetaldehyde in the dark on the TiO₂ film and P-25 powder was examined by injecting saturated gaseous acetaldehyde vapor into a sealed, air-filled container, and the decrease in acetaldehyde concentration via adsorption onto both the photocatalysts was meas-

ured gas-chromatographically on a Shimadzu Model GC-8A equipped with two 2 m Porapak-Q Columns, both with flame ionization detectors and one with an additional methanizer (see below), with nitrogen as the carrier gas. It should be noted that the adsorption measurements were carried out using the TiO₂ powder (referred to as TiO₂ powder A) from which the film was prepared, and not the TiO₂ film itself, because the total true surface area of the film was too small to be able to obtain precise adsorption parameters. Equilibrium was achieved at times of about 40–60 min after sample injection. The "adsorbed concentration" C_{ads} was calculated by subtracting the equilibrium concentration C_{eq} from the initial concentration C_0 . From an adsorption isotherm-type plot ($1/C_{\text{ads}}$ vs. $1/C_{\text{eq}}$), Langmuir adsorption parameters were calculated.

2.3. Photodecomposition studies

The photocatalytic activity of the film was evaluated by measuring the change in concentration of acetaldehyde and evolved CO₂ as a function of irradiation time. The photo-reactor vessel was made of Pyrex glass, with a volume of 1000 cm³. On the side exposed to the UV light, a transparent silica glass plate window (transmission 95% for UV light of wavelengths greater than 260 nm) was used. The distance of the TiO₂ film to the light source was about 25 cm, and a 4.5 × 4.5 cm square (about 20 cm² area) of the film was used. The UV intensity at the film surface was varied from 0.4 to 2.7 mW cm⁻². Similar experiments using TiO₂ powder A and commercial TiO₂ powder (Degussa P25, Nippon Aerosil Co. Ltd.) were also carried out. In this case, about 0.8 g of TiO₂ powder A and 0.25 g of P-25 powder were spread evenly on the bottom of a plastic dish (about 20 cm² area), and this was placed in the reaction vessel described above.

Saturated gaseous acetaldehyde was injected into the vessel so that the concentration was in the range of 300–2400 ppmv. Initially the vessel contained ambient air at a relative humidity of about 30–35%. The irradiations were conducted at room temperature after equilibrium between the gaseous and adsorbed acetaldehyde was reached (as ascertained by monitoring the concentration chromatographically about every 10 min). After starting the irradiation, the decrease in acetaldehyde concentration was also measured using the gas chromatograph, as described above. At the same time, the amount of gaseous carbon dioxide evolved was analyzed using the GC column which was equipped with the methanizer (Shimadzu, Model MTN-1), which was operated at a temperature of 400 °C.

The calculation of the quantum yields for the TiO₂ film as well as for P-25 powder was based on the number of absorbed photons within the photocatalyst layer. In this case, the light intensity absorbed in the layer is obtained by subtracting the transmitted light intensity (corrected for the absorbance of the fused silica substrate) from the incident light intensity.

3. Results and discussion

3.1. Structural properties

A relatively smooth, semi-transparent TiO₂ thin film, with a thickness of about 10 μm, was prepared on a glass substrate. SEM images are shown in Figs. 1(a) and 1(b), which show top and cross-sectional views, respectively. It can clearly be seen that, although the surface is relatively rough, the particles are well sintered. The film consists of small crystalline particles with an average diameter of about 50 nm. Because the average particle size in the sol was about 20 nm, it is assumed that the particles aggregated slightly during the heat treatment. The crystallographic characteristics were examined using X-ray diffraction and Raman spectroscopy, shown in Figs. 2 and 3, respectively. In the 2θ range from 20° to 60°, five peaks were observed: 25.2, 38.5, 48.0, 53.9 and 55.2. All of these peaks can be attributed to anatase [29]. No peaks other than those attributable to anatase were observed. The Raman spectroscopy also exhibited only bands that were attributable to anatase: 146, 397, 519 and 641 cm⁻¹ [30]. These observations show that, within the detection limits of the measurements, the film consisted of only anatase.

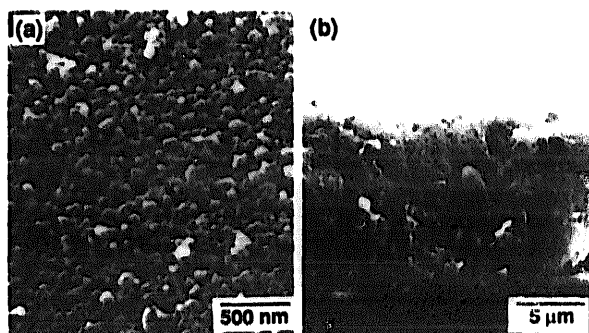


Fig. 1. SEM photomicrographs of (a) top and (b) cross-sectional views of the TiO₂ film.

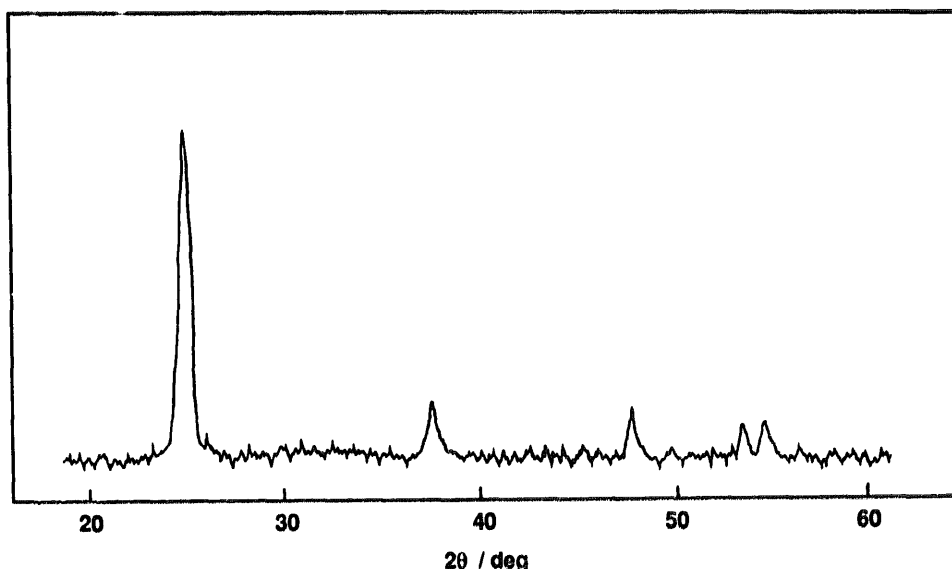


Fig. 2. X-Ray diffraction patterns of the TiO₂ film.

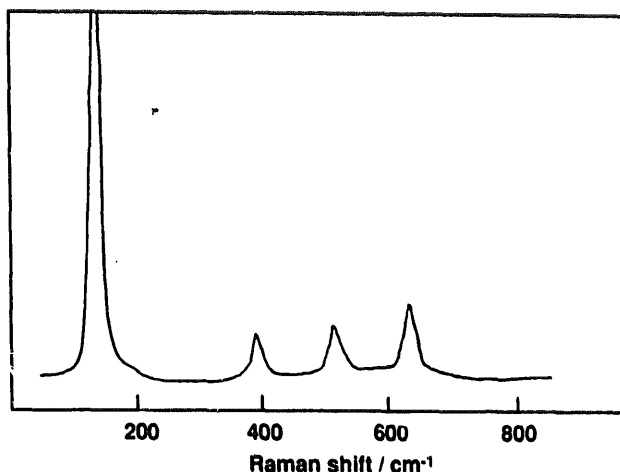


Fig. 3. Raman spectrum of the TiO₂ film.

3.2. Adsorption measurements

The adsorption properties of gas-phase acetaldehyde on TiO₂ powder A and P-25 powder were analyzed in terms of the Langmuir isotherm

$$\Theta = \frac{C_{\text{ads}}}{C_{\text{max}}} = \frac{KC_{\text{eq}}}{1 + KC_{\text{eq}}} \quad (2)$$

where Θ is the surface coverage, C_{ads} is the surface concentration of adsorbed molecules, C_{max} is the maximum surface concentration available for the adsorbate, K is the adsorption equilibrium constant, and C_{eq} is the equilibrium gas-phase concentration of the adsorbing species. Fig. 4 presents plots of the reciprocal of the "surface concentration" C_{ads}^{-1} vs. the reciprocal of the equilibrium concentration C_{eq}^{-1} for TiO₂ powder A and Degussa P-25 powder. The Langmuir isotherm parameters C_{max} and K were obtained using linear least-squares analysis and were found to be 100 μmol dm⁻³ and 0.016 dm³ μmol⁻¹, respectively, for TiO₂ powder A, and 17

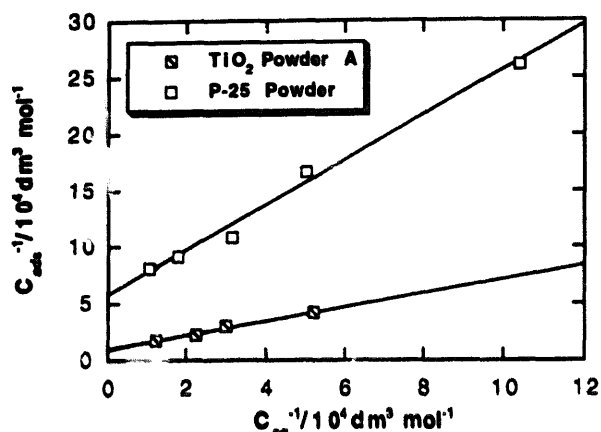


Fig. 4. Langmuir plots of the C_{ads}^{-1} vs. C_{eq}^{-1} for the adsorption of acetaldehyde gas on TiO_2 powder A and P-25 powder.

$\mu\text{mol dm}^{-3}$ and $0.030 \text{ dm}^3 \mu\text{mol}^{-1}$, respectively, for the P-25 powder. Considering the BET surface areas of TiO_2 powder A, $64 \text{ m}^2 \text{ g}^{-1}$, and P-25 powder, $50 \text{ m}^2 \text{ g}^{-1}$, as well as the weights of the TiO_2 powder (0.8 g) and P-25 powder (0.25 g) used, we obtained the maximum surface concentrations of acetaldehyde as $1.2 \text{ molecules nm}^{-2}$ and $0.8 \text{ molecules nm}^{-2}$ for TiO_2 powder A and P-25 powder, respectively¹. This result indicates that the adsorbability for gaseous acetaldehyde is slightly higher for TiO_2 powder A than for P-25 powder.

3.3. Photocatalytic reaction

Representative plots describing the decrease in the concentration of acetaldehyde (semilogarithmic plot) and the increase in the concentration of CO_2 (linear plot) as a function of time are shown in Figs. 5(a) and 5(b), respectively. These are results for photodegradation of 300 ppmv gaseous acetaldehyde in contact with the thin film, TiO_2 powder A and P-25 powder, with a UV intensity of 0.4 mW cm^{-2} . About 50 min after the injection of the reactant gas into the vessel, adsorption equilibrium was reached, and then the irradiation was started.

The initial decreases in the acetaldehyde concentrations showed apparent exponential decay, thus indicating first-order kinetics. It is clear from the figure that the TiO_2 film showed a higher photocatalytic activity than did the P-25 powder. The activity of the film was also somewhat higher than that of TiO_2 powder A. It should be noted, however, that although the apparent area of each catalyst was the same (20 cm^2) the weight of film used was approximately 40 times less than that of powder A. Thus it is clear that the activity of the film is also significantly higher than that of powder A. Similar results were also found for CO_2 production rates, as shown in Fig. 5(b).

¹ For the calculation method of the maximum surface concentration, see, for example, Ref. [31].

3.3.1. Kinetic analysis of the photodegradation of acetaldehyde

In order to elucidate the reasons for the high activity of the TiO_2 film, a Langmuir–Hinshelwood (L–H) kinetic model was used. The L–H model has been shown to provide a quantitative kinetic treatment of many solid–gas phase reactions [32]. This model includes the assumption that the Langmuir adsorption isotherm is valid for the surface reaction. The rate R of a unimolecular surface reaction will obey the following equation

$$R = k\theta = \frac{kKC_{\text{eq}}}{1 + KC_{\text{eq}}} \quad (3)$$

where k is the apparent first-order reaction rate constant.

Fig. 6 shows plots of the reciprocal of the initial degradation rate R^{-1} vs. the reciprocal of the equilibrium concentration of acetaldehyde C_{eq}^{-1} for degradation of acetaldehyde. The rate, R ($\text{mol dm}^{-3} \text{ min}^{-1}$), was calculated for the initial 20 min photo-irradiation time. The catalysts used were the TiO_2 thin film, TiO_2 powder A and Degussa P-25 powder, with a light intensity of 0.4 mW cm^{-2} . The plots are linear,

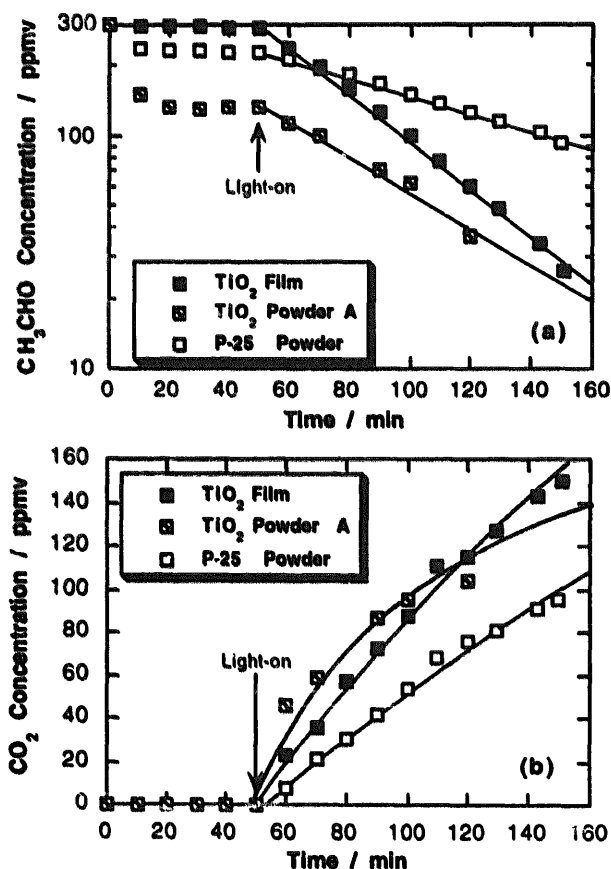


Fig. 5. Plots of (a) the decrease in acetaldehyde concentration and (b) the increase in CO_2 concentration vs. irradiation time during the photodegradation of 300 ppmv acetaldehyde gas in contact with the TiO_2 film, TiO_2 powder A, and P-25 powder under UV irradiation of 0.4 mW cm^{-2} intensity. The apparent area of each catalyst was the same (20 cm^2), with the weights used were 0.02 g, 0.8 g, and 0.25 g for the TiO_2 film, TiO_2 powder A and P-25 powder, respectively.

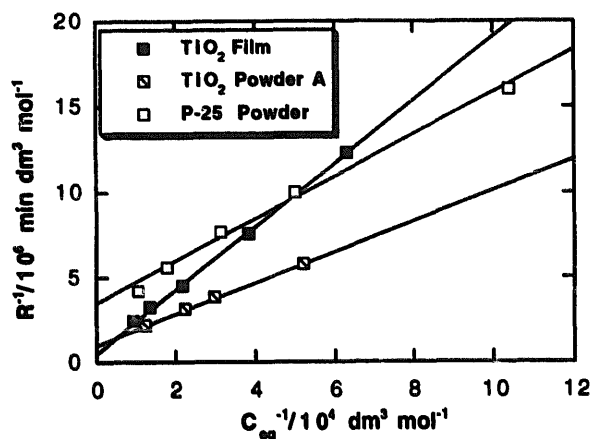


Fig. 6. Langmuir–Hinshelwood plots of R^{-1} vs. C_{eq}^{-1} for the degradation of acetaldehyde in contact with the TiO₂ film, TiO₂ powder A and P-25 powder under UV illumination of 0.4 mW cm⁻² intensity.

indicating that the treatment using the L–H model is appropriate for the photocatalytic acetaldehyde oxidation in contact with the three photocatalysts.

Analysis of the plot for the film provided L–H parameters of 1.50 $\mu\text{mol dm}^{-3} \text{ min}^{-1}$ and 0.0034 $\text{dm}^3 \mu\text{mol}^{-1}$ for k and K , respectively. The L–H parameters for powder A were 1.00 $\mu\text{mol dm}^{-3} \text{ min}^{-1}$ and 0.012 $\text{dm}^3 \mu\text{mol}^{-1}$ for k and K , respectively. Again, as discussed in connection with Fig. 5, although the rate constants are similar, the amount of TiO₂ in the film was a factor of 40 times less than that in the powder A sample used. Thus, if the rate constant is normalized to the weight of catalyst, the value for the film will be a factor of about 60 times higher than that for powder A. For P-25 powder, the k and K values were 0.30 $\mu\text{mol dm}^{-3} \text{ min}^{-1}$ and 0.028 $\text{dm}^3 \mu\text{mol}^{-1}$, respectively. It is also important to note that the values for the adsorption equilibrium constant for TiO₂ powder A (0.012 $\text{dm}^3 \mu\text{mol}^{-1}$) and P-25 powder (0.028 $\text{dm}^3 \mu\text{mol}^{-1}$) obtained from the kinetic analysis are in good agreement with those obtained from the adsorption analysis (0.016 $\text{dm}^3 \mu\text{mol}^{-1}$ for TiO₂ powder A and 0.030 $\text{dm}^3 \mu\text{mol}^{-1}$ for P-25 powder), thus confirming the validity of the L–H fitting.

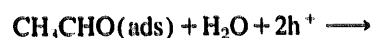
The reasons for the high photocatalytic activity of the anatase film have not been fully elucidated yet. However, one of the possible reasons is that, in addition to the relatively high surface area, the film may also have fewer defects (higher crystallinity) as a result of annealing at high temperature (450 °C). With a higher crystallinity, the number of electron–hole recombination centers would decrease. In this connection, it is also important to note that, in general, the crystallization of anatase causes a drastic decrease in the surface area [33]. However, in the case of our TiO₂ film, the heat treatment at 450 °C appears to have produced a surface with higher crystallinity but without a marked decrease in surface area. The autoclaving of the anatase sol at a relatively low temperature (180 °C) is considered to play a major role in this process by facilitating the subsequent crystallization.

Other possible reasons for the high activity of the film include differences in the efficiency for charge separation within the TiO₂ itself and in the efficiency for hole trapping by adsorbed reactants and intermediates. Other processes may also be involved, based on the possible reaction mechanisms (discussed later).

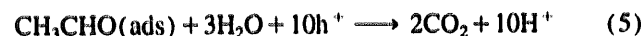
3.3.2. Dependences of quantum yield on light intensity and initial reactant concentration

The manner in which the quantum yields (QY) for acetaldehyde degradation were evaluated will now be described in detail. In the QY calculation, it should be noted that initial rates (after 10 min) of acetaldehyde disappearance and CO₂ production are used.

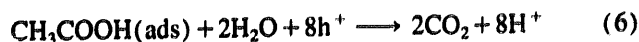
The oxidative photodegradation of acetaldehyde with a TiO₂ photocatalyst in principle proceeds as follows²:



and



When the number of molecules on the TiO₂ surface is much larger than the number of incident photons, most of the adsorbed acetaldehyde molecules should be oxidized to acetic acid (Eq. (4)). However, when the number of the holes photoproduced on the TiO₂ surface is much larger than the number of acetaldehyde molecules adsorbed, the proportion of direct oxidative conversion to CO₂ (Eq. (5)) might increase. Indeed, for a given set of experimental conditions, particularly a combination of low initial concentration of acetaldehyde and high UV intensity, the acetaldehyde degradation rate has been shown to parallel the CO₂ production rate, and it was also found that a stoichiometric yield of CO₂ could be obtained after the reaction was complete [34]. Suzuki also reported the same result using P-25 powder as the photocatalyst [35]. However, under the conditions reported here, the rate of CO₂ formation was lower than that of acetaldehyde degradation. This slower CO₂ formation compared to the acetaldehyde disappearance can be attributed to the relatively rapid formation of acetic acid as an intermediate, which subsequently oxidizes to CO₂ as shown in Eq. (6).



It is known that, in a deaerated aqueous solution, acetic acid converts to CO₂ and CH₄ in the presence of a TiO₂ photocatalyst via the so-called ‘photo-Kolbe reaction’

² Under the present experimental conditions, it was estimated and also found experimentally that the amount of water present in the ambient air was in at least a tenfold excess with respect to the amount needed to oxidize the acetaldehyde to CO₂ according to Fig. 5. For example, for an initial relative humidity of 32%, the relative humidity was found to decrease only by 2–5% relative humidity when the photocatalytic reaction was allowed to go essentially to completion.

Table 1
Quantum yields (QY) for photodegradation of gaseous acetaldehyde with the TiO₂ film and P-25 powder photocatalysts

| Initial conc. (ppmv) | UV intensity (mW cm ⁻²) | QY (%) | | Total |
|----------------------|-------------------------------------|-----------------|----------------------|-------|
| | | CO ₂ | CH ₃ COOH | |
| 1500 ^a | 0.4 | 68 | 50 | 118 |
| 1500 ^a | 2.7 | 93 | 23 | 116 |
| 300 ^a | 0.4 | 56 | 16 | 72 |
| 600 ^a | 0.4 | 50 | 6 | 56 |
| 1000 ^a | 0.4 | 47 | 12 | 59 |
| 2400 ^a | 0.4 | 98 | 26 | 124 |
| 600 ^b | 0.4 | 9 | 12 | 21 |
| 2400 ^b | 0.4 | 18 | 27 | 45 |

^a For the TiO₂ film.

^b For P-25 powder.

[36]. However, under the present conditions (ambient air), O₂ was present and can accept a conduction-band electron:



Thus the photo-Kolbe reaction scarcely occurs. Actually we did not observe CH₄ formation at all. The amounts of both acetic acid and CO₂ produced have to be known for the calculation of quantum yield. However, the quantitative analysis of acetic acid formation is difficult, because the acid may exist not only in the gas phase but also on the photocatalyst surface and on the reactor vessel walls. Therefore, the amount of acetic acid produced was estimated from the amount of acetaldehyde that had disappeared and the amount of evolved CO₂³. Under the assumption that only holes formed in the TiO₂ bulk were responsible for the formation of acetic acid and CO₂, the quantum yields for the reactions can be expressed as follows

$$\Phi_{\text{CH}_3\text{COOH}} = \frac{2 \times (\text{number of CH}_3\text{COOH produced})}{\text{number of photons absorbed on the catalyst surface}} \quad (8)$$

$$\Phi_{\text{CO}_2} = \frac{5 \times (\text{number of CO}_2 \text{ produced})}{\text{number of photons absorbed on the catalyst surface}} \quad (9)$$

and the total quantum yield is the sum of both.

Table 1 shows the relevant quantum yields for the photodegradation of acetaldehyde on the UV-illuminated TiO₂ film and P-25 powder photocatalysts, with different light intensities and initial reactant concentrations. It is clear from this table that the film showed higher photocatalytic activity than

³ Carbon dioxide can also be produced via photodegradation of acetic acid, but this process will be neglected because, as shown in Table 1, especially for the degradation by the film the quantum yields for CO₂ production are much higher than those for acetic acid production.

P-25 powder, as indicated by higher total quantum yields. Furthermore, the higher photoactivity of the film led to the observation that the quantum yields for CO₂ production were much higher than those for acetic acid production. Conversely, for the less active P-25 powder, the quantum yields for acetic acid production were higher than those for CO₂ production.

As expected on the basis of the preceding discussion, there was a tendency that the quantum yield for acetic acid formation decreased and that of CO₂ formation increased with increasing UV intensity at constant initial concentration. With a constant UV intensity of 0.4 mW cm⁻², the total quantum yield for the film ranged from 72 to 124% when the initial concentration was varied from 300 to 2400 ppmv. It is necessary to recall that these values were obtained by assuming that only photogenerated holes were responsible for the degradation of acetaldehyde. The values of the total quantum yield, which are greater than unity, indicate that the catalytic photo-oxidation did not proceed only via the simple initiation steps as assumed.

3.4. Mechanism of acetaldehyde photodegradation

It has been established that, when the TiO₂ semiconductor is irradiated with UV light of wavelength shorter than 380 nm, highly mobile electron-hole pairs can be created. These carriers, after migrating to the surface, can in turn be trapped by surface-adsorbed molecules at different sites, leading to oxidation and reduction processes. The hydroxyl radical is implicated as a reactive species in the photocatalyzed degradative oxidation of many organic compounds in liquid-solid systems as well as in gaseous phase systems. It is considered that the highly active radicals are formed through the capture of holes by surface water molecules and/or hydroxyl ions. At the same time free electrons, constantly generated in the conduction band by illumination, can be trapped by adsorbed oxygen, as shown in Eq. (7), forming O₂^{·-}. We have previously suggested [28] that the hydroxyl radicals generated solely by holes play a major role in the catalytic photodegradation of gaseous acetaldehyde. As widely recognized, the majority of the hydroxyl radicals formed in heterogeneous photocatalysis are derived from water [37], and therefore the reaction sequence of acetaldehyde oxidation can be described through the following equations



The net reaction is expressed in Eq. (4). Under strong UV irradiation, acetic acid formed will undergo further oxidation to CO₂, as described in Eq. (6). As was described in the previous section, however, the quantum yield calculated with Eqs. (4) and (5) exceeded 100%. Raupp and Junio [38] also reported that, in the photodegradative oxidation of gas-

eous-phase acetone and MTBE using P-25 powder in the presence of O₂, the apparent quantum yields were greater than 100%. (It should be noted that their calculation was based on *incident* light intensity, while ours was based on the *absorbed* intensity, but since, in our case, most of the light was absorbed by the film, the difference is not large.) These results imply that the acetaldehyde oxidation reactions are not exclusively mediated by hole-generated hydroxyl radicals. These authors [38] also observed the effect of increasing the O₂ concentration on the oxidation rates of gaseous reactants, although the effect became negligible for O₂ concentrations over 10 mol.%. One of the possible pathways is the direct oxidation of intermediate species by oxygen, as suggested by Schwitzgebel et al. for aqueous systems [39].

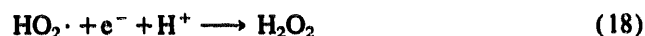


The total reaction is



Therefore, one hole oxidizes three acetaldehyde molecules, producing two acetic acid molecules and reactive radical CH₃CO·. Then the carbonyl radical is considered to play a main role in propagation of chain reactions.

An additional possibility is that the superoxide ion created by the conduction-band electron through Eq. (7) takes part in the oxidation reactions. For example, it is considered that H₂O₂ is formed from O₂^{•-} as follows [40]:



Actually, we have confirmed the production of H₂O₂ by the reduction of O₂ using a microelectrode technique [41]. Hydrogen peroxide production is subsequently followed by hydroxyl radical-forming reactions such as Eqs. (19) [42] and (20) [43]



or via direct photolysis [44],



The resultant ·OH radicals again play a major role in oxidizing acetaldehyde, as in Eqs. (11) and (12).

The superoxide radical itself has been suggested as being capable of reacting directly with adsorbed organic species on the TiO₂ surface, in the gaseous phase [45,46] as well as in

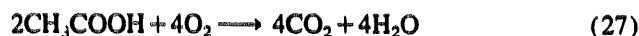
the aqueous phase [42]. Assuming the occurrence of direct contact between superoxide radicals and acetaldehyde molecules in the adsorbed state, the following reaction can be considered:



The total reaction is



Under strong illumination, further oxidation proceeds similarly.



We believe that all of these reaction sequences can contribute to quantum efficiencies larger than unity as calculated by Eqs. (8) and (9). Further investigation is in progress to estimate the proportions of hole-generated direct oxidation and of chain-reaction-contributed oxidation.

4. Summary

A glass-supported TiO₂ film with a particularly high photocatalytic effect was prepared by sintering an anatase sol at 450 °C. The film was relatively smooth and semitransparent. The photocatalytic activity of the film was investigated in terms of the photodegradative oxidation of gaseous acetaldehyde as a function of the UV light intensity. The TiO₂ film showed much higher photoactivity than Degussa P-25 TiO₂ powder, which is one of the most active known photocatalysts. The higher photocatalytic activity of the film can be attributed to a much higher-efficiency charge separation. The quantum yields, calculated on the basis of the number of absorbed photons and under the assumption that only photogenerated holes took part in the oxidative decomposition of the acetaldehyde, exceeded unity. Thus it is concluded that the acetaldehyde oxidation is not exclusively mediated by photogenerated holes but also by adsorbed oxygen, superoxide radicals and/or hydrogen peroxide. In addition, the oxidation process may involve a carbonyl-radical-mediated chain-reaction mechanism.

Acknowledgements

We express gratitude to Dr. D.A. Tryk for valuable discussions and careful reading of the manuscript. This work was supported by a Grant-in-Aid for Scientific Research from the Ministry of Education, Science and Culture of Japan.

References

- [1] A. Mills, R.H. Davies and D. Worsley, *Chem. Soc. Rev.*, 22 (1993) 417.
- [2] R.X. Cai, K. Hashimoto, Y. Kubota and A. Fujishima, *Chem. Lett.* (1992) 427.
- [3] M.A. Fox, *CHEMTECH*, 11 (1992) 680.
- [4] R.W. Matthew, *Sol. Energy*, 38 (1987) 405.
- [5] N. Kakuta, K.H. Park, M.F. Finlayson, A. Ueno, A.J. Bard, A. Campion, M.A. Fox, S.E. Webber and J.M. White, *J. Phys. Chem.*, 89 (1985) 1732.
- [6] D. Meissner, R. Memming and B. Kastening, *Chem. Phys. Lett.*, 96 (1983) 34.
- [7] M. Krishnan, J.M. White, M.A. Fox and A.J. Bard, *J. Am. Chem. Soc.*, 105 (1983) 7002.
- [8] A.W.H. Mau, C.B. Huang, N. Kakuta, A.J. Bard, A. Campion, M.A. Fox, J.M. White and S.E. Weber, *J. Am. Chem. Soc.*, 106 (1984) 6537.
- [9] E. Borgarello, N. Serpone, P. Liska, W. Erbs, M. Graetzel and E. Pelizzetti, *Gazz. Chim. Ital.*, 115 (1985) 599.
- [10] O. Enea and A.J. Bard, *J. Phys. Chem.*, 90 (1986) 301.
- [11] Y.M. Tricot and J.H. Fendler, *J. Am. Chem. Soc.*, 106 (1984) 2475.
- [12] Y.M. Tricot and J.H. Fendler, *J. Am. Chem. Soc.*, 106 (1984) 7359.
- [13] M. Meyer, C. Wallberg, K. Kurihara and J.H. Fendler, *J. Chem. Soc., Chem. Commun.*, (1980) 90.
- [14] N. Serpone, E. Borgarello, R. Harris, P. Cahill and M. Borgarello, *Sol. Energy Mater.*, 14 (1986) 121.
- [15] R.W. Matthew, *J. Phys. Chem.*, 91 (1987) 3328.
- [16] R.W. Matthew, *J. Catal.*, 111 (1988) 64.
- [17] S. Tunesi and M.A. Anderson, *J. Phys. Chem.*, 95 (1991) 3399.
- [18] J. Sabate, M.A. Anderson, H. Kikkawa, M. Edwards and C.G. Hill, *J. Catal.*, 127 (1991) 167.
- [19] J. Sabate, M.A. Anderson, H. Kikkawa, Q. Xu, S. Cervera-March and C.G. Hill, *J. Catal.*, 134 (1992) 36.
- [20] W. Lee, Y.M. Gao, K. Dwight and A. Wold, *Mat. Res. Bull.*, 27 (1992) 685.
- [21] Y.M. Gao, H.S. Shen, R.K. Dwight and A. Wold, *Mat. Res. Bull.*, 27 (1993) 1023.
- [22] A. Wold, *Chem. Mater.*, 5 (1993) 280.
- [23] J. Papp, H.S. Shen, R.K. Dwight and A. Wold, *Chem. Mater.*, 5 (1993) 284.
- [24] M.A. Aguardo and M.A. Anderson, *Sol. Energy Mater. Sol. Cell*, 28 (1993) 345.
- [25] H. Cui, H.S. Shen, Y.M. Gao, K. Dwight and A. Wold, *Mat. Res. Bull.*, 28 (1993) 195.
- [26] K. Vinodgopal, S. Hotchandani and P.V. Kamat, *J. Phys. Chem.*, 97 (1993) 9040.
- [27] H.S. Shen, Y. Gao, K. Dwight and A. Wold, *J. Solid State Chem.*, 106 (1993) 288.
- [28] I. Sopyan, S. Murasawa, K. Hashimoto and A. Fujishima, *Chem. Lett.*, (1994) 723.
- [29] Y.H. Chee, R.P. Cooney, R.F. Howe and P.A.W. van der Heide, *J. Raman Spectrosc.*, 23 (1992) 161.
- [30] G.J. Exarcos and N.J. Hess, *Thin Solid Films*, 220 (1992) 254.
- [31] J. Cunningham and G. Al-Sayyed, *J. Chem. Soc., Faraday Trans.*, 86 (1990) 3935.
- [32] P. Pichat and J.M. Herrmann, in N. Serpone and E. Pelizzetti (eds.), *Photocatalysis, Fundamentals and Applications*, Wiley, New York, 1989, p. 217.
- [33] I.A. Montoya, T. Viveros, J.M. Domingues, L.A. Canales and I. Schifter, *Catal. Lett.*, 15 (1992) 207.
- [34] I. Sopyan, S. Murasawa, K. Hashimoto and A. Fujishima, unpublished results.
- [35] K. Suzuki, *Trace. Met. Environ.*, 3 (1992) 421.
- [36] T. Sakata, in N. Serpone and E. Pelizzetti (eds.), *Photocatalysis, Fundamentals and Applications*, Wiley, New York, 1989, p. 328.
- [37] L.A. Dibble and G.B. Raupp, *Catal. Lett.*, 4 (1990) 345.
- [38] G.B. Raupp and C.T. Junio, *Appl. Surf. Sci.*, 72 (1993) 321.
- [39] J. Schwitzgebel, J.G. Ekerdt, H. Gerischer and Heller, *J. Phys. Chem.*, 99 (1995) 5633.
- [40] J.R. Harbour, J. Tromp and M.L. Hair, *Can. J. Chem.*, 63 (1985) 204.
- [41] H. Sakai, R. Baba, K. Hashimoto and A. Fujishima, *Trace Met. Environ.*, 3 (1993) 651.
- [42] I.M. Fraser and J.R. MacCallum, *J. Chem. Soc., Faraday Trans. 1*, 82 (1965) 2747.
- [43] M. Fujihira, Y. Satoh and T. Osa, *Bull. Chem. Soc. Jpn.*, 55 (1982) 666.
- [44] A.B. Ross, *J. Phys. Chem. Ref. Data*, 14 (1985) 1041.
- [45] R.I. Bickley and F.S. Stone, *J. Catal.*, 31 (1973) 389.
- [46] B. Ohtani, Y. Ueda, S. Nishimoto, T. Kagiya and H. Hachisuka, *J. Chem. Soc., Perkin Trans.*, 2 (1990) 1955.